

1 **Title:** Early life stress affects the miRNA cargo in epididymal extracellular vesicles in
2 mouse

3

4 **Authors:** Anar Alshanbayeva^{1,2,3}, Deepak K. Tanwar^{1,2,3}, Martin Roszkowski^{1,2,3}, Francesca
5 Manuella^{1,2,3}, Isabelle M. Mansuy^{1,2,3*}

6 **Affiliations:** ¹Laboratory of Neuroepigenetics, Brain Research Institute, Medical Faculty of
7 the University of Zurich, Zurich, Switzerland; ²Institute for Neuroscience, Department of
8 Health Sciences and Technology, ETH Zurich, Zurich, Switzerland; ³Zurich Neuroscience
9 Center, ETH Zurich and University of Zurich, Zurich, Switzerland

10

11 **Running title:** Early life stress changes epididymosomal miRNAs

12 **Summary Sentence:** miRNA cargo of extracellular vesicles in cauda epididymis is changed
13 by paternal exposure to early life stress, which correlates with differences in the expression
14 of their target genes in sperm and zygotes generated from that sperm

15

16 **Keywords:** epigenetics; epididymis, miRNAs, epididymosomes, early life stress, sperm,
17 extracellular vesicles.

18 **Grant support:** The work was supported by Swiss National Science Foundation (31003A-
19 135715), ETH grants (ETH-10 15-2 and ETH-17 13-2), the Slack-Gyr foundation, the Escher
20 Foundation.

21 **Correspondence to:** Isabelle M. Mansuy; Tel: +41 44 635 3360; E-mail:
22 mansuy@hifo.uzh.ch; Winterthurerstrasse 190, CH-8057 Zürich

23 **Abstract**

24 Sperm RNA can be modified by environmental factors and has been implicated in
25 communicating signals about changes in a father's environment to the offspring. The RNA
26 composition of sperm is influenced during its final stage of maturation in the epididymis by
27 extracellular vesicles released by epididymal cells. We studied the effect of exposure to
28 stress in postnatal life on the transcriptome of epididymal extracellular vesicles using a
29 mouse model of transgenerational transmission. We found that the small RNA signature of
30 epididymal extracellular vesicles, particularly miRNAs, is altered in adult males exposed to
31 postnatal stress. miRNAs changes correlate with differences in the expression of their
32 target genes in sperm and zygotes generated from that sperm. These results suggest that
33 stressful experiences in early life can have persistent biological effects on the male
34 reproductive tract that may in part be responsible for the transmission of the effects of
35 exposure to the offspring.

36

37 **Introduction**

38 Post-testicular maturation of spermatozoa in the epididymis is an elaborate process
39 that involves modifications of sperm RNA, protein and lipid content [1–5]. The epididymis is
40 segmented into different parts, including the initial segment, caput, corpus and cauda.
41 Each segment has a distinct gene expression profile, and different protein and lipid
42 composition. Some modifications in epididymal spermatozoa are conserved across species
43 [6]. For example, approximately 50% of miRNAs, a class of small RNAs that are modified
44 during caput to cauda epididymis transit, is identical in mouse and bovine spermatozoa [6].
45 One mechanism by which small RNA load in spermatozoa is modified along the epididymis
46 is by uptake of extracellular vesicles (EVs), also known as epididymosomes, which are
47 produced by epididymal epithelial cells [7]. Studies have shown that epididymosomes can

48 be taken up by maturing sperm through proteins present on the sperm head such as
49 dynamin in mice and tetraspanins or syntenins in humans [7–10]. Co-incubation
50 experiments provided evidence for epididymosome-mediated transfer of miRNAs to
51 spermatozoa [7]. Exogenous DNA and RNA can also be directly taken up by spermatozoa
52 via artificial liposomes [11].

53 However, it is still not clear if changes in small RNA composition of spermatozoa
54 occurring during epididymal transit are required for embryonic development, and studies
55 on the subject have been conflicting [12,13]. Changes in sperm small RNA have
56 nevertheless been suggested to play a role in the transmission of information about
57 paternal experiences to the progeny and can influence their developmental trajectory
58 [2,14,15]. Epididymosomal small RNA content can also be altered by exposure, for instance,
59 to dietary insult or stress [2,14]. For instance, epididymosomal miRNAs are changed by
60 exposure to chronic stress [14] and low-protein diet [2] in mice.

61 Transmission of information about paternal exposure to the offspring depends on
62 the type of exposure, as well as on its duration and developmental window [16]. To date,
63 little is known about the long-term effects of early life stress, particularly stress
64 experienced after birth on epididymosomal small RNA composition in adulthood and
65 whether any change can influence gene expression in sperm and in zygotes generated
66 from that sperm. Using a transgenerational mouse model of postnatal stress (based on
67 unpredictable maternal separation combined with unpredictable maternal stress, MSUS)
68 [17], we show that the miRNA signature of cauda epididymosomes in adult males is altered
69 by exposure to postnatal stress. The alterations in miRNA composition are found to
70 correlate with changes in the expression of targets of these miRNAs in sperm and zygotes.

71

72 **Results**

73 **Isolation of cauda epididymosomes confirmed by several methods**

74 To characterize RNA composition of cauda epididymosomes, epididymosomes were
75 first isolated from adult control males and adult males exposed to MSUS by high-speed
76 ultracentrifugation (Figure 1A). Successful isolation of cauda epididymosomes was
77 confirmed by electron microscopy, immunoblotting and nanoparticle-tracking analyses
78 (Figure 1). The presence and purity of epididymosomes was further validated by staining
79 with the EV-specific marker CD9 and absence of the cellular marker GAPDH (Figure 1B).
80 Size analysis by nanoparticle-tracking indicated that the collected particles are 50-300 nm
81 in diameter (Figure 1D), and imaging by transmission electron microscopy showed the
82 typical cup-shaped structures of epididymosomes (Figure 1C, Supplementary Figure 1A)
83 [18]. RNA profiling by high-resolution automated electrophoresis showed enrichment for
84 small RNAs of different lengths, similar to previous studies on cauda epididymosomal RNA
85 content (Supplementary Figure 1B) [2,13].

86

87 **The number and size of epididymosomes in adult males are not altered by postnatal
88 stress**

89 We next examined the number and size of epididymosomes in adult MSUS and
90 control males by dynamic light scattering. No significant difference in the number or mean
91 size of cauda epididymosomes could be detected between MSUS and control males (Figure
92 2A, 2B). Since most epididymosomal secretion occurs via apocrine secretion from principal
93 cells located in caput epididymis, we also examined the level of expression of genes
94 involved in extracellular vesicles secretion. We chose Ras-related protein Rab-5A (*Rab5*) and
95 Ras-related protein Rab-7A (*Rab7*), which are involved in vesicle trafficking, the SNARE

96 family protein vesicle-associated membrane protein 7 (*Vamp7*) and SNARE recognition
97 molecule synaptobrevin homolog YKT6 (*Ykt6*), involved in vesicle fusion. No significant
98 change in the expression of these genes could be detected in caput epididymis between
99 MSUS and control mice, despite a consistent trend for decreased expression in MSUS mice
100 (Figure 2C).

101

102 **miRNAs are persistently altered by postnatal stress in cauda epididymosomes**

103 Epididymosomal small RNAs are known to be affected by changing environmental
104 conditions in rodents. Small RNAs, like tRNA-derived fragments (tRFs) are believed to act
105 as messengers of a father's experiences to the offspring [2,14]. Our previous work showed
106 that early postnatal stress alters small and long RNA content in sperm in adult males [15].
107 Since caudal sperm and epididymosomal small RNA profiles are highly similar [2], we
108 examined whether small RNA content of cauda epididymosomes is also altered by
109 postnatal stress. RNA of different sizes was observed in cauda epididymosomes, with the
110 majority of small RNA reads mapping to tRNAs as previously observed (Figure 3A) [2].
111 When plotting the top different small RNAs between the two groups, the majority of small
112 RNA differences between MSUS and control epididymosomes appeared to be in miRNAs
113 (Figure 3B). Therefore, we performed size-selection on the same libraries and re-sequenced
114 them to enrich for miRNAs (Supplementary Figure 2A, 2C). As expected, size-selection did
115 not alter the abundance of different miRNAs and uniformly enriched the miRNA fraction in
116 all samples (Supplementary Figure 2B, 2C, 2D). Pathway analysis of small RNA-sequencing
117 (sRNA-seq) datasets after size-selection revealed that the most up-regulated and down-
118 regulated miRNAs ($P < 0.05$) in MSUS cauda epididymosomes have target mRNAs that
119 encode proteins involved in pathways, including fatty acid metabolism, steroid

120 biosynthesis, lysine degradation and thyroid hormone signaling (Figure 3C). Notably,
121 similar pathways are altered in plasma of MSUS males as shown by unbiased metabolomic
122 analysis that we previously conducted [19]. In particular, metabolites implicated in
123 polyunsaturated fatty acid biogenesis were up-regulated, whereas steroidogenesis and the
124 steroidogenic ligand aldosterone were down-regulated in circulation of MSUS males [19].
125 These results suggest systemic changes in fatty acid metabolism and steroidogenesis
126 pathways in adult MSUS males. Notably, steroidogenesis was already altered during
127 postnatal life in MSUS males with total cholesterol significantly decreased in testis, while
128 HDL cholesterol was significantly increased in liver in MSUS males at postnatal day 28
129 (Figure 3D, 3F). Since the primary role of HDL cholesterol in blood is to transport excess
130 cholesterol from peripheral tissues and lipoproteins to the liver, an increase in HDL in the
131 liver corresponds to the HDL decrease in testis. However, cholesterol was no longer altered
132 in testis of adult MSUS males (Figure 3E), suggesting a transient alteration. The androgen
133 receptor, that binds androgens which are derived from cholesterol, showed however a
134 trend for decreased expression in adult caput epididymis (Figure 3G), suggesting potential
135 secondary effects of lower cholesterol in testis earlier in life.

136

137 **mRNA targets of miRNAs from cauda epididymosomes are altered by postnatal stress**
138 **in sperm and zygotes**

139 The relative abundance of miRNAs in cauda epididymosomes and mature sperm
140 was significantly correlated (Figure 4C), consistent with previous results [2]. Since cauda
141 epididymosomes carry small RNA payloads matching those of mature sperm and are part
142 of the ejaculate [20,21], they may contribute to the information delivered to the embryo.
143 Therefore, we looked at the mRNA targets of the miRNAs significantly changed in MSUS

144 cauda epididymosomes (adjusted $P \leq 0.05$), which include miR-871-5p, miR-31-5p, miR-155-
145 5p and miR34c-5p, among differentially expressed genes we previously identified in MSUS
146 sperm and zygotes ($P < 0.05$) [15,22]. For this, we plotted the cumulative log fold-change
147 distribution of genes versus the different numbers of conserved binding sites for these
148 miRNAs (Figure 4A and 4B, Supplementary Figure 5). Target genes with 3 binding sites for
149 miR-31-5p, a miRNA differentially expressed in MSUS cauda epididymosomes, had
150 increased expression in sperm and decreased expression in zygotes from MSUS males
151 (Figure 4A, 4B). However, not all targets of significantly altered miRNAs from MSUS cauda
152 epididymosomes showed corresponding expression changes in sperm and zygotes
153 (Supplementary Figure 5). We performed miRNA-gene interaction analysis based on
154 experimentally validated data from Tarbase [23]. From this analysis, we identified that the
155 5 miRNAs significantly changed in MSUS cauda epididymosomes target genes that are part
156 of pathways involved in steroid biosynthesis, ECM-receptor interaction and cell adhesion
157 molecules (Figure 4D).

158

159 Discussion

160 The effects of environmental factors on RNA in the male reproductive tract, in
161 particular, the epididymis have been examined in rodent models. Until now, most models
162 have used invasive exposure such as dietary insult and injection of endocrine disruptors and
163 their effects when applied prenatally and sometimes even before conception. Very few
164 studies have examined the effects of non-invasive psychological/emotional exposure such
165 as stress in early life and the effects on epididymal RNA in adulthood. This study addresses
166 the question of whether postnatal stress affects RNA in the epididymis and whether this
167 has consequences for sperm in adulthood and zygotes generated from that sperm.

168 Using a transgenerational mouse model of early postnatal stress, we show that
169 several miRNAs including miR-871-3p, miR-31-5p, miR-155-5p, miR-878-5p and miR-34c-5p
170 are altered in the epididymis of adult males exposed to stress and that the targets of some
171 of these miRNAs are affected in mature sperm and zygotes. Particularly, miR-31-5p is
172 significantly decreased in cauda epididymosomes from exposed males and its target genes
173 are increased in sperm. Interestingly, these genes are decreased in zygotes generated from
174 that sperm (Figure 4B), suggesting a possible over-compensation during early
175 development. This may also be due to the heterogeneity of epididymosomes which have
176 different size, biogenesis and cellular targeting [24], leading to a dissociation between the
177 RNA content of epididymosomes and transcriptional changes in the zygotes (Figure 4A, 4B
178 and Supplementary Figure 5). It has been suggested that a subset of epididymosomes can
179 communicate with spermatozoa during its epididymal transit [2,7], another subset serves in
180 the communication within epididymal epithelial cells [25], and a third subset is delivered as
181 part of seminal fluid during fertilization [20,21]. Therefore, due to their heterogeneity, not
182 all cauda epididymosomes or their cargo may be delivered to the oocyte upon fertilization,
183 which may explain the differences in miRNAs targets between sperm and zygotes.

184 Several of the differentially expressed miRNAs in MSUS cauda epididymosomes
185 play a role in metabolic processes and early development [26]. For instance, miR-31-5p is
186 involved in glucose metabolism and fatty acid oxidation [26]. In *A. japonicus*, its target
187 complement C1q Tumor Necrosis Factor-Related Protein 9A (*CTRP9*) protein is negatively
188 associated with the amount of visceral fat and is positively associated with a favourable
189 glucose or metabolic phenotype [27]. Alterations in glucose and insulin metabolism are also
190 characteristic of MSUS mice [15,17]. Other miRNAs significantly changed in MSUS
191 epididymosomes, such as miR-155-5p, which facilitates differentiation of mouse embryonic

192 stem cells, whereas miR-34c-5p is thought to initiate the first embryonic cleavage in mice
193 [26].

194 The first days after birth are a sensitive period for the development and
195 establishment of tissue-specific niches for several tissues. Epithelial cells, which are the
196 source of epididymosomes in the epididymis, undergo differentiation and expansion
197 postnatally until puberty [28]. Upon completing the expansion, the number of epididymal
198 epithelial cells remains nearly constant in adulthood, thus possibly carrying a memory of
199 early life exposure into adulthood. The postnatal development and differentiation of
200 epididymal epithelial cells primarily depend on testicular signals [28–31]. Since long-term
201 stress affects the coupling of the hypothalamus-pituitary and hypothalamus-gonadal axes,
202 stress-related decrease in steroidogenesis can have profound effects on the differentiation
203 and expansion of epididymal epithelial cells in early postnatal life. A number of studies have
204 shown the importance of the abundance of androgens during postnatal life for epididymal
205 development [29]. Thus, the availability of testicular cholesterol during the differentiation
206 of epididymal epithelial cells has implications for these cells. Systemic alteration in
207 cholesterol metabolism seen in young MSUS males (decreased total cholesterol in testis
208 and increased HDL cholesterol in the liver) may contribute to the metabolic changes seen in
209 adult animals, such as changes in plasma metabolome of steroidogenesis and fatty acid
210 pathways, as well as alterations in glucose and insulin metabolism in adult MSUS males.
211 Moreover, androgen-dependent miRNAs miR-878-5p and miR-871-3p are significantly
212 increased in cauda epididymosomes in MSUS.

213 In conclusion, our results provide evidence that chronic stress exerted immediately
214 after birth alters miRNAs in extracellular vesicles of the male reproductive tract until
215 adulthood, with effects in mature sperm and zygotes. Such persistent and

216 intergenerational effects *in vivo* point to the sensitivity of the reproductive system to stress
217 exposure and the detrimental consequences for descendants. These consequences likely
218 differ depending on the time window and severity of paternal stress exposure. Further
219 studies will be necessary to determine these effects as well as the source of the vesicles and
220 their cargo miRNAs.

221

222 **Materials and Methods**

223 **Animals**

224 Animal experiments were conducted according to the Swiss Law for Animal Protection and
225 were approved by the cantonal veterinary office in Zürich under license number 83/2018.
226 C57Bl/6J mice were obtained from Janvier (France) and bred in-house to generate animals
227 for the experiments. Animals were maintained under a reverse light-dark cycle in a
228 temperature and humidity-controlled environment with constant access to food and
229 water.

230

231 **MSUS**

232 To obtain MSUS mice, 3-month old C57Bl/6J dams and their litters were randomly split into
233 MSUS and Control groups. MSUS dams and their litters were subjected to daily 3 hour
234 separation and a stressor as previously described [17], while control dams and pups were
235 left undisturbed. After weaning at postnatal day 21, pups from different dams were
236 randomly assigned to cages of 4-5 mice, in corresponding treatment groups to avoid litter
237 effects.

238

239 **Tissue collection**

240 After decapitation and blood collection, mice were pinned on a dissection board and
241 cleaned with alcohol. Epididymis and testis were carefully excised and separated from
242 surrounding adipose tissue. The epididymis was further separated into caput, corpus and
243 cauda. Cauda was excised with several incisions and sperm collected with a swim-up
244 protocol. The supernatant was collected to isolate epididymosomes. The whole testis and
245 caput epididymis were crushed with stainless steel beads in a tissue crusher in cold PBS,
246 centrifuged at 3'000 rcf for 10 min to pellet the tissue and cells and used for total
247 cholesterol and HDL cholesterol measurements.

248

249 **Electron microscopy images**

250 Negative staining of cauda epididymosomes was performed with methylcellulose. Briefly,
251 the carrier grid was glow-discharged in plasma for 10 min and washed with a drop of PBS,
252 then incubated in 1% glutaraldehyde (GA) in water for 5 min and washed with water 5 times
253 for 2 min each. Afterwards the grid was incubated in 1% UAc (uranyl acetate) for 5 min and
254 then kept on ice in Methylcellulose/UAc (900 µl Methylcellulose 2 % and 100 µl 3 % UAc)
255 solution. After incubation with Methylcellulose/UAc, the excess liquid was removed by
256 dipping onto a filter paper. The grid was air-dried on ice for 5 min. Imaging was performed
257 with a Transmission Electron Microscope.

258

259 **Epididymosome isolation by ultracentrifugation and density-gradient**

260 After pelleting sperm following the sperm swim-up protocol in M2 medium (Sigma, M7167),
261 the supernatant was centrifuged at 2'000 rcf for 10 min, 10'000 rcf for 30 min and then
262 ultracentrifuged at 120'000 rcf at 4 °C for 2 h (TH 64.1 rotor, Thermo Fisher Scientific). The
263 epididymosomal pellet was then washed in PBS at 4 °C and ultracentrifuged at 120'000 rcf

264 at 4 °C for 2 h. The resulting pellet was resuspended in 60 µl of PBS for all downstream
265 analysis.

266

267 Immunoblotting

268 The PBS-resuspended pellet containing epididymosomes was lysed in 10x RIPA buffer for 5
269 min at 4 °C. Equal amounts of protein were mixed with 4x Laemmli Sample Buffer (Bio-Rad
270 Laboratories, USA) and loaded on 4-20% Tris-Glycine polyacrylamide gels (Bio-Rad
271 Laboratories, USA). The membranes were blocked in 5% SureBlock (in Tris-buffer with
272 0.05% Tween-20) for 1 h at room temperature and incubated with primary antibodies
273 overnight at 4 °C with anti-*Cd9* ([1:3000; System Biosciences, Palo Alto, CA, USA] and anti-
274 *Gapdh* [1:5000; Cell Signaling, Davers, MA, USA; 14C10]).

275

276 Nanoparticle tracking analysis

277 Particle number and size of epididymosomes were measured using a Nanosight NS300
278 (Malvern, UK) at 20 °C, according to the manufacturer's instructions and lots were
279 generated using a published method [32]. The following parameters were kept constant for
280 all samples: "Camera level" = 14 and "Detection threshold" = 7. For measurements with
281 Nanosight, the resuspended pellet from ultracentrifugation was diluted to a 1:1000
282 concentration.

283

284 RNA isolation and epididymosomes profiling

285 To lyse purified epididymosomes, 33 µl of lysis buffer (6.4 M guanidine HCl, 5 % Tween 20, 5
286 % Triton, 120 mM EDTA, and 120 mM Tris pH 8.0) per every 60 µl of PBS resuspended
287 pellet was added to each sample, together with 3.3 µl ProteinaseK and 3.3 µl of water.

288 Samples were incubated at 60 °C for 15 min with shaking. 40 µl of water was added and
289 RNA was extracted using the Trizol LS protocol, according to the manufacturer's
290 instructions. Profiling of the extracted RNA was performed using high-resolution
291 automated electrophoresis on a 2100 Bioanalyzer (Agilent, G2939BA), according to
292 instructions for the RNA 6000 Pico Kit (Agilent, 5067-1513) reagent.

293

294 **Preparation and sequencing of small RNA-seq libraries from epididymosomes**

295 sRNA-seq libraries were prepared using the NEB Next Small RNA-sequencing kit (NEB
296 #E7300, New England BioLabs), according to the manufacturer's instructions. 80-90 ng of
297 total RNA per sample was used to prepare the libraries. The same libraries were sequenced
298 before and after size-selection (target peak 150bp) with the BluePippin System. 200 million
299 reads were obtained for 10 samples, with 125bp single-stranded read-length on a
300 HiSeq2500 sequencer.

301

302 **RT-qPCR**

303 For gene expression analysis in caput epididymis, RNA was extracted using the
304 phenol/chloroform extraction method (TRIzol; Thermo Fisher Scientific). Reverse
305 transcription was performed using miScript II RT reagents (Qiagen) - HiFlex buffer, and RT
306 qPCR was performed with QuantiTect SYBR (Qiagen) on the Light-Cycler II 480 (Roche). All
307 samples were run in cycles as follows: 95 °C for 15 min, 45 cycles of 15 sec at 94 °C, 30 sec at
308 55 °C and 30 sec at 70°C, followed by gradual increase of temperature to 95 °C. The
309 endogenous control *Gapdh* was used for normalization. Primer sequences for individual
310 genes are made available in the Supplementary Table 1. The expression level of genes was
311 analysed using two-tailed Student's t-test.

312

313 **Cholesterol measurements**

314 Testicular and epididymal total cholesterol and HDL cholesterol levels were measured using
315 the CHOL reagent, in conjunction with SYNCHRON LX® System(s), UniCel® DxC 600/800
316 System(s) and Synchron® Systems Multi Calibrator (Beckman Coulter), according to the
317 manufacturer's instructions at the Zurich Integrative Rodent Physiology (ZIRP) facility of
318 the University of Zurich.

319 **Bioinformatics data analysis**

320 Small RNA-sequencing FASTQ files were processed using the ExceRpt pipeline, a
321 previously established pipeline for extracellular vesicle small RNA data analysis [33]. Briefly,
322 ExceRpt first automatically identifies and removes known 3' adapter sequences. Afterwards
323 the pipeline aligns against known spike-in sequences used for library construction, filters
324 low-quality reads and aligns them to annotated sequences in the UniVec database and
325 endogenous ribosomal RNAs. Reads that were not filtered out in the pre-processing steps
326 are then aligned to the mouse genome and transcriptome using STAR aligner [34]. The
327 annotations were performed in the following order: miRbase, tRNAscan, piRNA, GENCODE
328 and circRNA. Reads mapped to miRNAs were combined from sequencing obtained before
329 and after size-selection and were corrected for batch effect using RUVSeq [35].
330 Normalization factors were calculated using the TMM [36] method and differential
331 expression was performed using the edgeR package [37] in R.

332 For cumulative distribution plots, miRNA targets (all and conserved) were downloaded
333 from TargetScan release 7.2 [38]. When using the context++ scores, targets were split into 3
334 same-frequency groups according to their scores. *P*-values were calculated using a
335 Kolmogorov-Smirnov test between the first and the last groups (i.e., strongest and weakest

336 targets). The miRNA pathway analysis was conducted using a web-server tool DIANA-
337 miRPath [23], where targets were predicted-derived from DIANA-TarBase v6.0, a database
338 of experimentally validated miRNA targets. The adjusted *P* cutoff value of 0.05 was used
339 for the identification of expressed pathways. The miRNAs and their corresponding target
340 pathways information was extracted and plots were generated in R. ggplot2 [39] and
341 ComplexHeatmap [40] R packages were used for generation of figures.

342

343 **Data availability**

344 The datasets collected for this study are available as follows:

- 345 • sRNA-seq dataset of epididymosomes before size-selection :
346 • sRNA-seq dataset of epididymosomes after size-selection :
347 • Codes used for bioinformatics analysis of the RNA-sequencing datasets:

348

349 **Acknowledgements**

350 We thank Pierre-Luc Germain for advice on data analysis and for generating cumulative
351 distribution plots, Irina Lazar-Contes for help with MSUS breeding, Silvia Schelbert for work
352 on the animal license, Emilio Yandez at Function Genomics Center Zurich (FGCZ) for advice
353 on the small RNA sequencing, Alekhya Mazumkhar for help with nanoparticle-tracking
354 analysis, Yvonne Zipfel for animal care, Zurich Integrative Rodent Physiology facility for
355 performing cholesterol measurements. We also thank Eloise Kremer, Ali Jawaid and Mea
356 Holmes for their initial contributions to the project. The Mansuy lab is funded by the
357 University Zürich, the Swiss Federal Institute of Technology, the Swiss National Science
358 Foundation (31003A-135715), ETH grants (ETH-10 15-2 and ETH-17 13-2), the Slack-Gyr
359 foundation, the Escher Foundation. Deepak K. Tanwar is supported by the Swiss

360 Government Excellence Scholarship. Martin Roszkowski was funded by the ETH Zurich
361 Fellowship (ETH-10 15-2).

362

363

364 **Authors contributions**

365 AA and IMM conceived and designed the study. FM and MR performed the MSUS breeding
366 and collected tissue samples. AA and DKT performed data analysis and generated figures.
367 AA wrote the manuscript with input from DKT and IMM. AA performed all experiments for
368 RNA sequencing and all molecular analyses. IMM supervised the project and raised funds.

369

370 **Conflict of interest**

371 The authors declare no conflict of interest.

372

373 **Main Figure panel legends**

374 **Figure 1.**

375 **Isolation and characterization of cauda epididymosomes (A)** Schematic representation
376 of cauda epididymosomes preparation. **(B)** Immunoblot analysis was used to confirm the
377 purity of isolations by staining with epididymosomal marker CD9 and absence of cellular
378 marker GAPDH in the ultracentrifuged pellet. **(C)** Electron microscopy images of the
379 preparations were used to access the size and heterogeneity of the isolated populations.
380 **(D)** Nanoparticle-tracking analysis by dynamic light scattering showed isolation of particles
381 of expected size of 50-300 nm.

382

383 **Figure 2.**

384 **Comparison of epididymosomal number, size and release machinery in MSUS and**
385 **control. (A)** Nanoparticle-tracking analysis showed no difference in the number of cauda
386 epididymosomes between MSUS and control males. The plots were generated from
387 average values across replicates (N = 5 animals/group). Data are presented as mean ±
388 standard error of the mean (SEM). $P < 0.05$. **(B)** Quantification of nanoparticle-tracking
389 analysis showed the mean size of cauda epididymosomes was not changed between the
390 two groups (N = 5 animals/group). Data are presented as mean ± SEM. $P < 0.05$. **(C)**
391 Expression of genes involved in vesicular secretion in the caput epididymis from adult males
392 measured by qRT-PCR. The experiments were performed in triplicates without pooling (N =
393 8 animals/group). Expression of Gapdh was used as endogenous control to normalize the
394 expression level of the target genes. Data are presented as mean ± SEM. $P < 0.05$.

395

396 **Figure 3.**

397 **Target pathways of up- and down-regulated miRNAs in MSUS cauda epididymosomes.**
398 **Alterations in steroidogenesis in MSUS males. (A)** Representative distribution of RNA
399 biotypes from cauda epididymosomal sequencing (N = 10 animals, 5 animals/group). **(B)**
400 Heatmap of the most abundant small RNAs (n = 39). Expression fold-change (\log_2 FC) was
401 calculated by subtracting \log_2 counts per million (CPM) of MSUS from Controls. Each row
402 depicts a small RNA and each column depicts a sample. Samples and RNAs are ordered by
403 "PCA" method using seriation (R package). **(C)** Dot plot of miRNAs and pathways. Color-
404 scale of the dot represents $-\log_{10}$ adjusted P of miRNA in a pathway and size of the dot
405 represents $-\log_{10}$ adjusted P of the pathway. Total cholesterol measurements in whole
406 testes of males at postnatal day 28 (N = 4 males/group) **(D)** or adulthood (N = 10 Controls, N

407 = 7 MSUS) (**E**). (**F**) HDL cholesterol level in the liver of males at postnatal day 28 (N = 6
408 males/group). (**G**) Relative expression level of the androgen receptor in adult caput
409 epididymis measured by qRT-PCR. qRT-PCR experiments were performed in triplicates,
410 without pooling (N = 10 animals/group). (**D, E, F, G**) Data are presented as mean ± standard
411 error of the mean (SEM). $P < 0.05$.

412

413

414 **Figure 4.**

415 **Targets of miRNAs from cauda epididymosomes are altered by postnatal stress in**
416 **sperm and zygotes**

417 Cumulative distribution plots of miR-31-5p targets in differentially expressed genes ($P <$
418 0.05) from MSUS sperm RNA-seq (**A**) and zygote RNA-seq (**B**). (**C**) miRNA abundance of
419 sperm plotted against abundance in cauda epididymosomes. Coefficient of determination
420 (R^2) = 0.74. (**D**) Dot plot of the top target pathways (adjusted $P < 0.05$) of miRNAs
421 differentially expressed (adjusted $P \leq 0.05$) in MSUS cauda epididymosomes. Color-scale of
422 the dot represents $-\log_{10}$ adjusted P of miRNA in a pathway and size of the dot represents -
423 \log_{10} adjusted P of the pathway.

424

425 **Supplementary Figure Panels**

426

427 **Supplementary Figure 1.**

428 (A) Electron microscopy images of the preparations were used to access the size and
429 heterogeneity of the isolated populations. (B) The RNA amount of epididymosomes
430 preparations was assessed by high-resolution automated electrophoresis.

431

432 **Supplementary Figure 2.**

433 (A) RNA read-length distributions of cauda epididymosomal small RNAs after size-
434 selection. (B) Heatmap of top miRNAs of cauda epididymosomal small RNA-seq before and
435 after size-selection. Each row depicts a miRNA and each column depicts a sample. (N= 10
436 Controls, N=10 MSUS). (C) Representative distribution of RNA biotypes from cauda
437 epididymosomal small RNA-seq after size-selection. (N = 5 Controls, N = 5 MSUS). (D)
438 miRNA abundance distributions plot of cauda epididymosomal small RNA-seq. (N = 10
439 Controls, N = 10 MSUS)

440

441 **Supplementary Figure 3.**

442 Scatterplot of log fold-change of miRNAs in sperm and cauda epididymosomes. miRNAs
443 down-regulated (blue) and up-regulated (red) in MSUS cauda epididymosomes.

444

445

446 **Supplementary Figure 4.**

447 Profiles of cauda epididymosomal small RNAs by high-resolution automated
448 electrophoresis. (N = 10 Controls, N = 10 MSUS).

449

450 **Supplementary Figure 5.**

451 Cumulative distribution plots of miR-34c-5p, miR-155-5p targets in differentially expressed
452 genes ($P < 0.05$) from MSUS sperm and zygote RNA-sequencing.

453

454 **Supplementary Figure 6.**

455 Immunoblot images of cauda epididymosomes and liver cell lysate, stained with cellular
456 marker GAPDH (37kDa) and extracellular vesicle marker CD9 (25kDa). Same membrane
457 was incubated and imaged separately.

458

459

460

461 **Bibliography**

462 [1] Tamessar CT, Trigg NA, Nixon B, Skerrett-Byrne DA, Sharkey DJ, Robertson SA,
463 Bromfield EG, Schjenken JE. Roles of male reproductive tract extracellular vesicles in
464 reproduction. Am J Reprod Immunol n.d.; 85:e13338.

465 [2] Sharma U, Conine CC, Shea JM, Boskovic A, Derr AG, Bing XY, Belleannee C,
466 Kucukural A, Serra RW, Sun F, Song L, Carone BR, et al. Biogenesis and function of tRNA
467 fragments during sperm maturation and fertilization in mammals. Science 2016; 351:391–
468 396.

469 [3] Nixon B, Stanger SJ, Mihalas BP, Reilly JN, Anderson AL, Tyagi S, Holt JE,
470 McLaughlin EA. The microRNA signature of mouse spermatozoa is substantially modified
471 during epididymal maturation. Biol Reprod 2015; 93:91.

- 472 [4] Rejraji H, Sion B, Prensier G, Carreras M, Motta C, Frenoux J-M, Vericel E, Grizard G,
473 Vernet P, Drevet JR. Lipid remodeling of murine epididymosomes and spermatozoa during
474 epididymal maturation. *Biol Reprod* 2006; 74:1104–1113.
- 475 [5] Skerget S, Rosenow MA, Petritis K, Karr TL. Sperm proteome maturation in the
476 mouse epididymis. *PLoS ONE* 2015; 10:e0140650.
- 477 [6] Sellem E, Marthey S, Rau A, Jouneau L, Bonnet A, Perrier J-P, Fritz S, Le Danvic C,
478 Boussaha M, Kiefer H, Jammes H, Schibler L. A comprehensive overview of bull sperm-
479 borne small non-coding RNAs and their diversity across breeds. *Epigenetics Chromatin*
480 2020; 13:19.
- 481 [7] Reilly JN, McLaughlin EA, Stanger SJ, Anderson AL, Hutcheon K, Church K, Mihalas
482 BP, Tyagi S, Holt JE, Eamens AL, Nixon B. Characterisation of mouse epididymosomes
483 reveals a complex profile of microRNAs and a potential mechanism for modification of the
484 sperm epigenome. *Sci Rep* 2016; 6:31794.
- 485 [8] Caballero JN, Frenette G, Belleannée C, Sullivan R. CD9-positive microvesicles
486 mediate the transfer of molecules to Bovine Spermatozoa during epididymal maturation.
487 *PLoS ONE* 2013; 8:e65364.
- 488 [9] Thimon V, Frenette G, Saez F, Thabet M, Sullivan R. Protein composition of human
489 epididymosomes collected during surgical vasectomy reversal: a proteomic and genomic
490 approach. *Hum Reprod* 2008; 23:1698–1707.
- 491 [10] Zhou W, Stanger SJ, Anderson AL, Bernstein IR, De Iuliis GN, McCluskey A,
492 McLaughlin EA, Dun MD, Nixon B. Mechanisms of tethering and cargo transfer during
493 epididymosome-sperm interactions. *BMC Biol* 2019; 17:35.
- 494 [11] Bachiller D, Schellander K, Peli J, Rüther U. Liposome-mediated DNA uptake by
495 sperm cells. *Mol Reprod Dev* 1991; 30:194–200.

- 496 [12] Suganuma R, Yanagimachi R, Meistrich ML. Decline in fertility of mouse sperm with
497 abnormal chromatin during epididymal passage as revealed by ICSI. *Hum Reprod* 2005;
498 20:3101–3108.
- 499 [13] Conine CC, Sun F, Song L, Rivera-Pérez JA, Rando OJ. Small RNAs Gained during
500 Epididymal Transit of Sperm Are Essential for Embryonic Development in Mice. *Dev Cell*
501 2018; 46:470-480.e3.
- 502 [14] Chan JC, Morgan CP, Adrian Leu N, Shetty A, Cisse YM, Nugent BM, Morrison KE,
503 Jašarević E, Huang W, Kanyuch N, Rodgers AB, Bhanu NV, et al. Reproductive tract
504 extracellular vesicles are sufficient to transmit intergenerational stress and program
505 neurodevelopment. *Nat Commun* 2020; 11:1499.
- 506 [15] Gapp K, Jawaid A, Sarkies P, Bohacek J, Pelczar P, Prados J, Farinelli L, Miska E,
507 Mansuy IM. Implication of sperm RNAs in transgenerational inheritance of the effects of
508 early trauma in mice. *Nat Neurosci* 2014; 17:667–669.
- 509 [16] Fennell KA, Busby RGG, Li S, Bodden C, Stanger SJ, Nixon B, Short AK, Hannan AJ,
510 Pang TY. Limitations to intergenerational inheritance: subchronic paternal stress
511 preconception does not influence offspring anxiety. *Sci Rep* 2020; 10:16050.
- 512 [17] Franklin TB, Russig H, Weiss IC, Gräff J, Linder N, Michalon A, Vizi S, Mansuy IM.
513 Epigenetic transmission of the impact of early stress across generations. *Biol Psychiatry*
514 2010; 68:408–415.
- 515 [18] Choi H, Mun JY. Structural analysis of exosomes using different types of electron
516 microscopy. *AM* 2017; 47:171–175.
- 517 [19] van Steenwyk G, Gapp K, Jawaid A, Germain P-L, Manuella F, Tanwar DK, Zamboni
518 N, Gaur N, Efimova A, Thumfart KM, Miska EA, Mansuy IM. Involvement of circulating

- 519 factors in the transmission of paternal experiences through the germline. *EMBO J* 2020;
520 39:e104579.
- 521 [20] Frenette G, Légaré C, Saez F, Sullivan R. Macrophage migration inhibitory factor in
522 the human epididymis and semen. *Mol Hum Reprod* 2005; 11:575–582.
- 523 [21] Belleannée C, Légaré C, Calvo E, Thimon V, Sullivan R. microRNA signature is
524 altered in both human epididymis and seminal microvesicles following vasectomy. *Hum*
525 *Reprod* 2013; 28:1455–1467.
- 526 [22] Gapp K, van Steenwyk G, Germain PL, Matsushima W, Rudolph KLM, Manuella F,
527 Roszkowski M, Vernaz G, Ghosh T, Pelczar P, Mansuy IM, Miska EA. Alterations in sperm
528 long RNA contribute to the epigenetic inheritance of the effects of postnatal trauma. *Mol*
529 *Psychiatry* 2020; 25:2162–2174.
- 530 [23] Vlachos IS, Hatzigeorgiou AG. Functional Analysis of miRNAs Using the DIANA
531 Tools Online Suite. *Methods Mol Biol* 2017; 1517:25–50.
- 532 [24] Sullivan R. Epididymosomes: a heterogeneous population of microvesicles with
533 multiple functions in sperm maturation and storage. *Asian J Androl* 2015; 17:726–729.
- 534 [25] Belleannée C, Calvo É, Caballero J, Sullivan R. Epididymosomes convey different
535 repertoires of microRNAs throughout the bovine epididymis. *Biol Reprod* 2013; 89:30.
- 536 [26] Reza AMMT, Choi Y-J, Han SG, Song H, Park C, Hong K, Kim J-H. Roles of
537 microRNAs in mammalian reproduction: from the commitment of germ cells to peri-
538 implantation embryos. *Biol Rev Camb Philos Soc* 2019; 94:415–438.
- 539 [27] Shao Y, Li C, Xu W, Zhang P, Zhang W, Zhao X. miR-31 Links Lipid Metabolism and
540 Cell Apoptosis in Bacteria-Challenged *Apostichopus japonicus* via Targeting CTRP9. *Front*
541 *Immunol* 2017; 8:263.

- 542 [28] Robaire B, Hinton BT (eds.). *The epididymis: from molecules to clinical practice.*
543 Boston, MA: Springer US; 2002.
- 544 [29] Robaire B, Hamzeh M. Androgen action in the epididymis. *J Androl* 2011; 32:592–
545 599.
- 546 [30] Zhu LJ, Hardy MP, Inigo IV, Huhtaniemi I, Bardin CW, Moo-Young AJ. Effects of
547 androgen on androgen receptor expression in rat testicular and epididymal cells: a
548 quantitative immunohistochemical study. *Biol Reprod* 2000; 63:368–376.
- 549 [31] Bilińska B, Wiszniewska B, Kosiniak-Kamysz K, Kotula-Balak M, Gancarczyk M,
550 Hejmej A, Sadowska J, Marchlewicz M, Kolasa A, Wenda-Różewicka L. Hormonal status of
551 male reproductive system: androgens and estrogens in the testis and epididymis. *In vivo*
552 and *in vitro* approaches. *Reprod Biol* 2006; 6 Suppl 1:43–58.
- 553 [32] Dragovic RA, Gardiner C, Brooks AS, Tannetta DS, Ferguson DJP, Hole P, Carr B,
554 Redman CWG, Harris AL, Dobson PJ, Harrison P, Sargent IL. Sizing and phenotyping of
555 cellular vesicles using Nanoparticle Tracking Analysis. *Nanomedicine* 2011; 7:780–788.
- 556 [33] Rozowsky J, Kitchen RR, Park JJ, Galeev TR, Diao J, Warrell J, Thistlethwaite W,
557 Subramanian SL, Milosavljevic A, Gerstein M. exceRpt: A Comprehensive Analytic Platform
558 for Extracellular RNA Profiling. *Cell Syst* 2019; 8:352–357.e3.
- 559 [34] Dobin A, Davis CA, Schlesinger F, Drenkow J, Zaleski C, Jha S, Batut P, Chaisson M,
560 Gingeras TR. STAR: ultrafast universal RNA-seq aligner. *Bioinformatics* 2013; 29:15–21.
- 561 [35] www.biorxiv.org/content/10.1101/006585v2.full.pdf.
562 <https://www.biorxiv.org/content/10.1101/006585v2.full.pdf>. Accessed February 26, 2021.
- 563 [36] Robinson MD, Oshlack A. A scaling normalization method for differential
564 expression analysis of RNA-seq data. *Genome Biol* 2010; 11:R25.

- 565 [37] Robinson MD, McCarthy DJ, Smyth GK. edgeR: a Bioconductor package for
566 differential expression analysis of digital gene expression data. *Bioinformatics* 2010;
567 26:139–140.
- 568 [38] Agarwal V, Bell GW, Nam J-W, Bartel DP. Predicting effective microRNA target
569 sites in mammalian mRNAs. *Elife* 2015; 4.
- 570 [39] Create Elegant Data Visualisations Using the Grammar of Graphics • *ggplot2*.
571 <https://ggplot2.tidyverse.org/>. Accessed March 5, 2021.
- 572 [40] Gu Z, Eils R, Schlesner M. Complex heatmaps reveal patterns and correlations in
573 multidimensional genomic data. *Bioinformatics* 2016; 32:2847–2849.

Figure 1. bioRxiv preprint doi: <https://doi.org/10.1101/2021.04.29.441964>; this version posted April 29, 2021. The copyright holder for this preprint (which was not certified by peer review) is the author/funder, who has granted bioRxiv a license to display the preprint in perpetuity. It is made available under aCC-BY-NC-ND 4.0 International license.

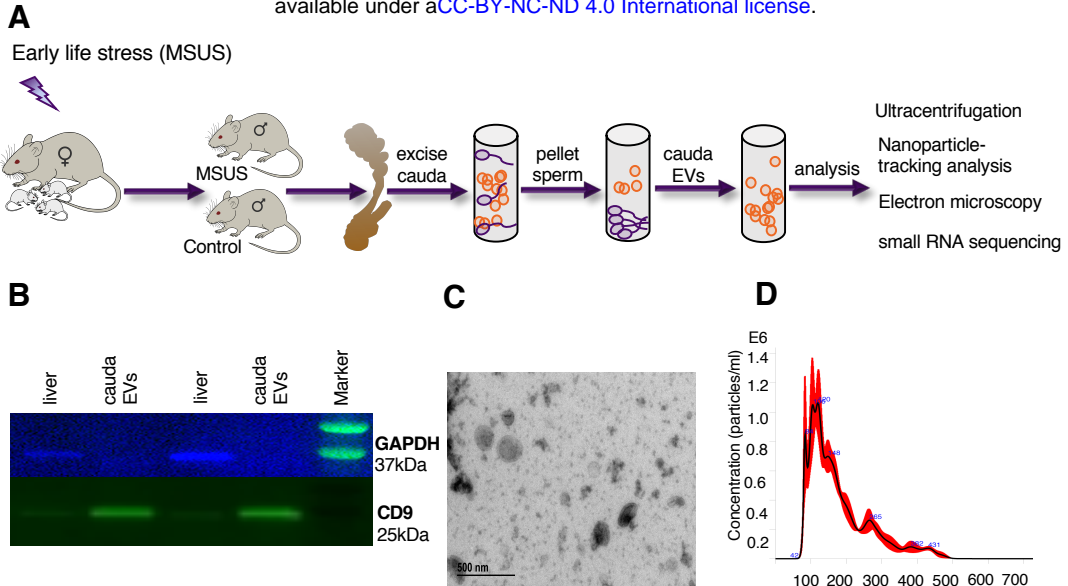


Figure 2.

bioRxiv preprint doi: <https://doi.org/10.1101/2021.04.29.441964>; this version posted April 29, 2021. The copyright holder for this preprint (which was not certified by peer review) is the author/funder, who has granted bioRxiv a license to display the preprint in perpetuity. It is made available under aCC-BY-NC-ND 4.0 International license.

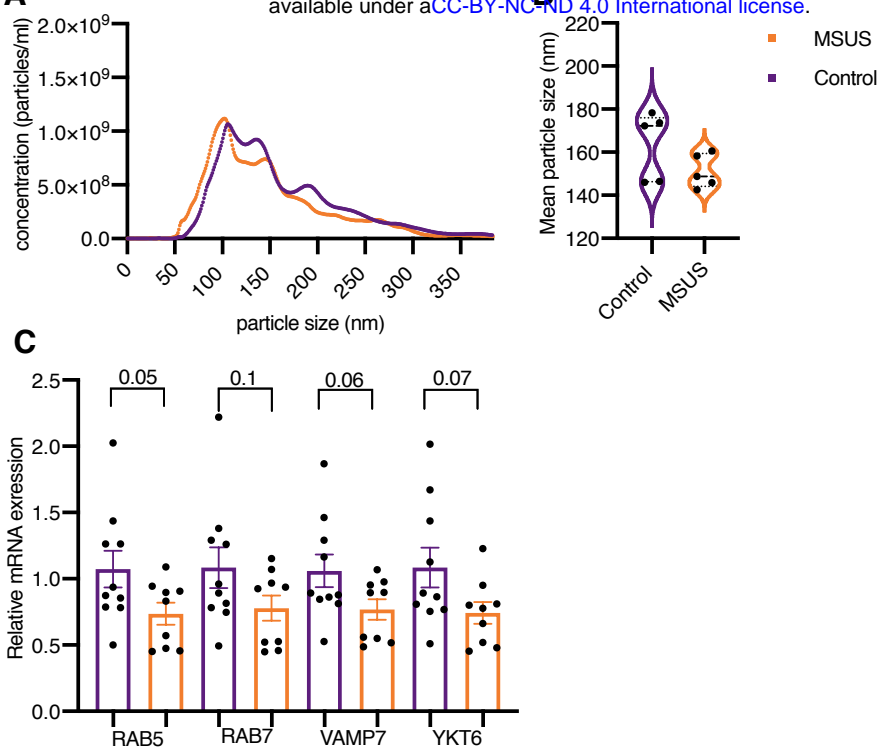
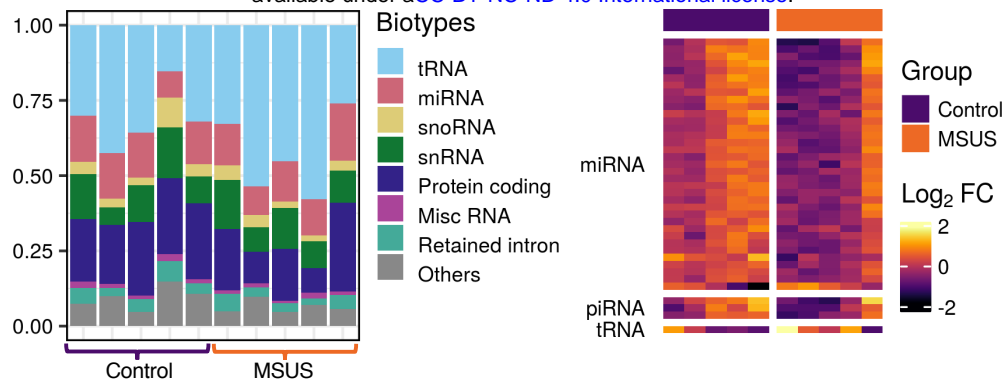
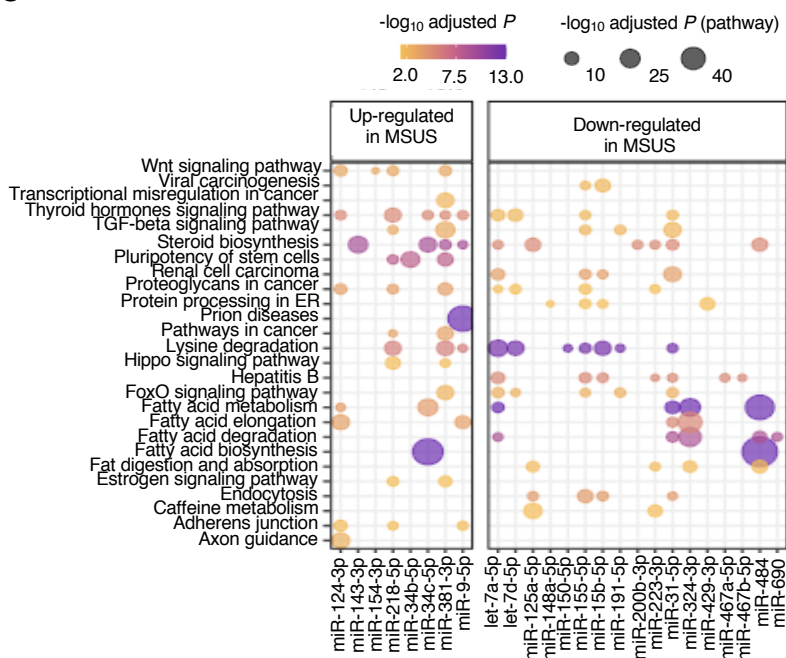
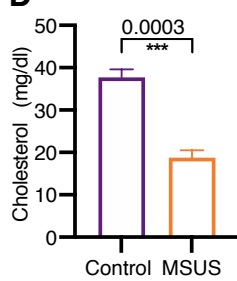
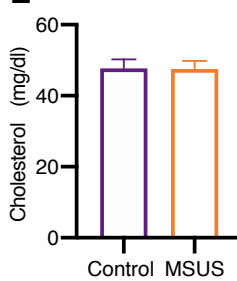
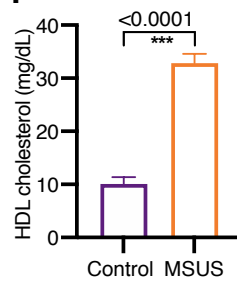
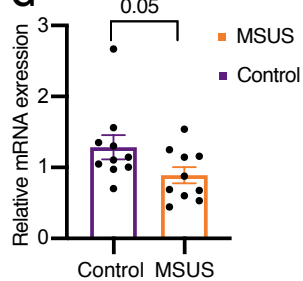
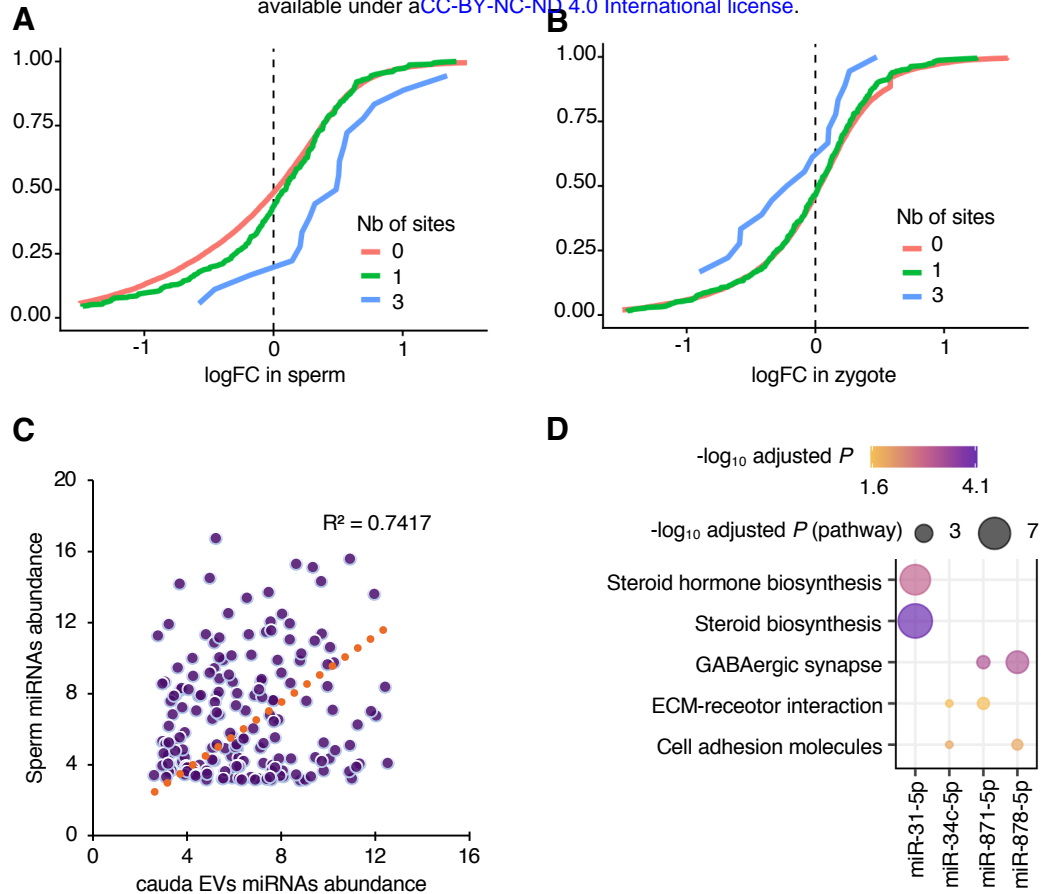


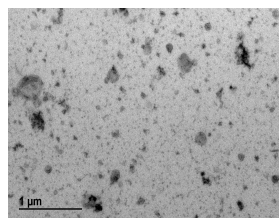
Figure 3.

bioRxiv preprint doi: <https://doi.org/10.1101/2021.04.29.441964>; this version posted April 29, 2021. The copyright holder for this preprint (which was not certified by peer review) is the author/funder, who has granted bioRxiv a license to display the preprint in perpetuity. It is made available under aCC-BY-NCND 4.0 International license.

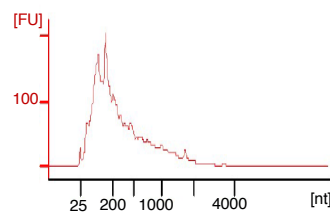
A**C****D****E****F****G**



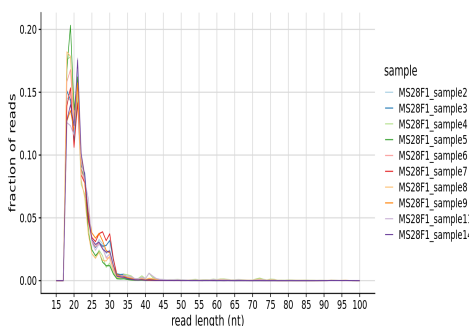
A



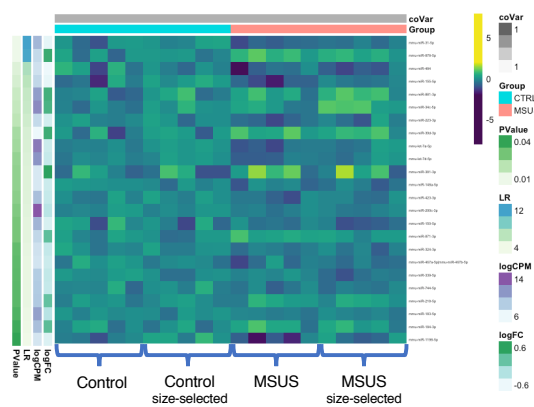
B



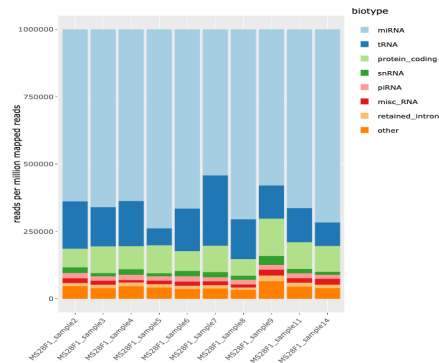
A



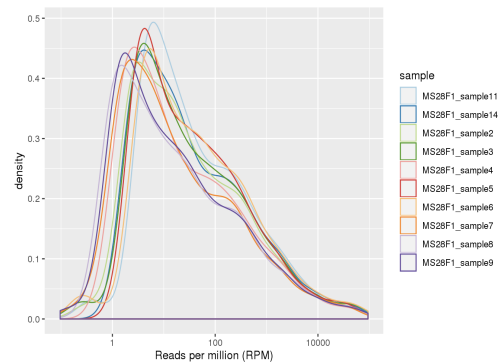
B

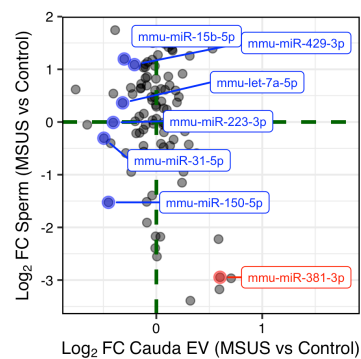


C



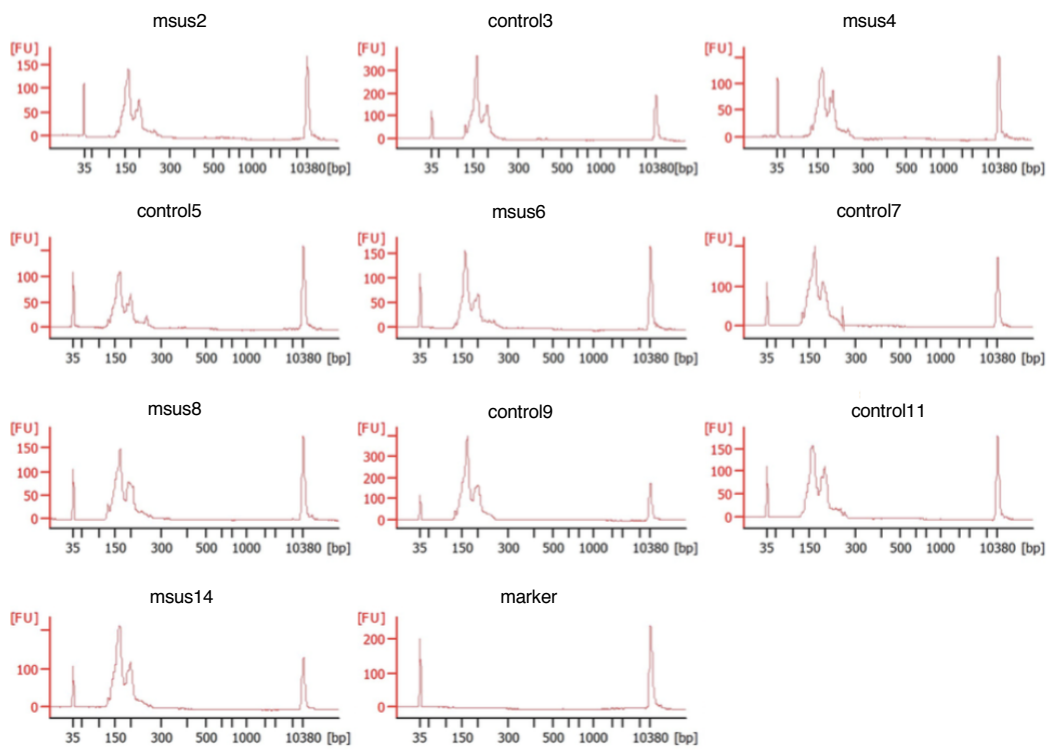
D





Supplementary Figure 4

bioRxiv preprint doi: <https://doi.org/10.1101/2021.04.29.441964>; this version posted April 29, 2021. The copyright holder for this preprint (which was not certified by peer review) is the author/funder, who has granted bioRxiv a license to display the preprint in perpetuity. It is made available under aCC-BY-NC-ND 4.0 International license.



Supplementary Figure 5

bioRxiv preprint doi: <https://doi.org/10.1101/2021.04.29.441964>; this version posted April 29, 2021. The copyright holder for this preprint (which was not certified by peer review) is the author/funder, who has granted bioRxiv a license to display the preprint in perpetuity. It is made available under aCC-BY-NC-ND 4.0 International license.

